



Differential response of vegetation in Hulun Lake region at the northern margin of Asian summer monsoon to extreme cold events of the last deglaciation

Shengrui Zhang ^{a, b}, Jule Xiao ^{a, b, c, *}, Qinghai Xu ^d, Ruilin Wen ^a, Jiawei Fan ^a, Yun Huang ^{a, b}, Hideki Yamagata ^e

^a Key Laboratory of Cenozoic Geology and Environment, Institute of Geology and Geophysics, Chinese Academy of Sciences, Beijing 100029, China

^b College of Earth and Planetary Sciences, University of Chinese Academy of Sciences, Beijing 100049, China

^c CAS Center for Excellence in Life and Paleoenvironment, Beijing 100044, China

^d College of Resources and Environment, Hebei Key Laboratory of Environmental Change and Ecological Construction, Hebei Normal University, Shijiazhuang 050024, China

^e Paleo Labo Co., Ltd., Saitama 335-0016, Japan

ARTICLE INFO

Article history:

Received 20 December 2017

Received in revised form

2 April 2018

Accepted 25 April 2018

Available online 7 May 2018

Keywords:

Last deglaciation

Extreme cold event

East Asia

Hulun lake

Pollen

Regional vegetation

ABSTRACT

The response of vegetation to extreme cold events during the last deglaciation is important for assessing the impact of possible extreme climatic events on terrestrial ecosystems under future global warming scenarios. Here, we present a detailed record of the development of regional vegetation in the northern margin of Asian summer monsoon during the last deglaciation (16,500–11,000 cal yr BP) based on a radiocarbon-dated high-resolution pollen record from Hulun Lake, northeast China. The results show that the regional vegetation changed from subalpine meadow-desert steppe to mixed coniferous and deciduous forest-typical steppe during the last deglaciation. However, its responses to the Heinrich event 1 (H1) and the Younger Dryas event (YD) were significantly different: during the H1 event, scattered sparse forest was present in the surrounding mountains, while within the lake catchment the vegetation cover was poor and was dominated by desert steppe. In contrast, during the YD event, deciduous forest developed and the proportion of coniferous forest increased in the mountains, the lake catchment was occupied by typical steppe. We suggest that changes in Northern Hemisphere summer insolation and land surface conditions (ice sheets and sea level) caused temperature and monsoonal precipitation variations that contributed to the contrasting vegetation response during the two cold events. We conclude that under future global warming scenarios, extreme climatic events may cause a deterioration of the ecological environment of the Hulun Lake region, resulting in increased coniferous forest and decreased total forest cover in the surrounding mountains, and a reduction in typical steppe in the lake catchment.

© 2018 Elsevier Ltd. All rights reserved.

1. Introduction

As the principal component of terrestrial ecosystems, vegetation plays a crucial role in sustaining the global carbon cycle, regulating greenhouse gas concentrations and influencing regional climates (Bonan et al., 1992; Schimel, 1995). Therefore, the response

processes and feedback mechanisms of vegetation to climate change have been a major focus of global change research (e.g. Lashof et al., 1997). The last deglaciation was punctuated by several abrupt climatic events in high northern latitudes that had a major influence on global atmospheric circulation and terrestrial ecosystems (Denton et al., 2010; Clark et al., 2012). Thus, understanding vegetation succession and its response to abrupt climatic events during the last deglaciation in different regions is important for assessing the impact of future global warming and possible extreme climatic events on terrestrial ecosystems.

Previous studies have shown that the vegetation composition changed significantly in Europe (Huntley, 1990; Binney et al., 2017),

* Corresponding author. Institute of Geology and Geophysics, Chinese Academy of Sciences, No. 19, Beitucheng Western Road, Chaoyang District, 100029, Beijing, China.

E-mail address: jlxiao@mail.iggcas.ac.cn (J. Xiao).

North America (Prentice et al., 1991; Williams et al., 2002) and the tropics (Hughen et al., 2004) during the last deglaciation: during the Bølling-Allerød warming event (B/A) and the early Holocene, forest expanded at low latitudes (Hughen et al., 2004) and horizontal vegetation zones migrated northward and inland in mid-high latitudes (Huntley, 1990; Williams et al., 2002; Dyke, 2005). In contrast, during the Heinrich event 1 (H1) and the Younger Dryas event (YD), forest shrank and dry grassland dominated at low latitudes (Hughen et al., 2004), while cold-resistant species increased at mid-high latitudes (Yu and Eicher, 1998). These observations indicated that the vegetation responded rapidly and sensitively to abrupt climate change, but that the changes in vegetation communities and the extent and rate of migration of vegetation zones varied significantly at different latitudes.

Vegetation change in East Asia during the last deglaciation has received much research attention in recent years (Demske et al., 2005; Stebich et al., 2009; Park and Park, 2015; Wu et al., 2016a, 2016b). It is well established that the vegetation responded dramatically to millennial- and centennial-scale climatic fluctuations during this period (Stebich et al., 2009; Park and Park, 2015; Wu et al., 2016a). However, most of the previous studies have focused on mountain lakes or small lakes (e.g., Sihailongwan Lake - Stebich et al., 2009; Hanon Maar paleolake - Park and Park, 2015; Moon Lake - Wu et al., 2016a; and Gonghai Lake - Xu et al., 2017) which are significantly affected by factors such as lake basin shape, topography, and altitude. Consequently, such records tend to reflect variations in local vegetation or vertical migration of mountain vegetation zones (Jacobson and Bradshaw, 1981; Sugita, 1994) and they provide less information about changes in regional vegetation. In addition, existing high-resolution paleo-vegetation records mainly came from low-middle latitudes and there is a dearth of records from higher latitudes of East Asia. Therefore, there is a need for a greater number of regional paleo-vegetation records from mid-high latitudes to provide a more comprehensive understanding of the vegetation response to extreme cold events during the last deglaciation.

Hulun Lake is in a climatically sensitive region, on the north-eastern edge of the current monsoon margin, and therefore is well suited for reconstructing regional climate and vegetation change (Xiao et al., 2009; Wen et al., 2010). In this study, we reconstructed the vegetation history of the Hulun Lake region during the last deglaciation (16,500–11,000 cal yr BP) based on AMS ^{14}C dating and pollen analysis. Our aims were to determine the response of the regional vegetation at the northern margin of Asian summer monsoon to abrupt climate change, with the focus on the extreme cold events of H1 and YD. It was hoped that the results would provide insights into the possible regional vegetation response to future global warming and associated extreme climatic events.

2. Hulun Lake and its environment

Hulun Lake (48°30'40" to 49°20'40"N, 117°00'10" to 117°41'40"E, 543 m a.s.l.) is located ca. 30 km south of Manchuria, Inner Mongolia, in an inland graben basin that formed in the late Pliocene (Fig. 1A). The Hulun Lake has a catchment of 37,214 km² within the borders of China, and two major rivers enter the lake, the Herlun River (more than 1000 km long) flowing from the south-eastern part of the Hentiy Mountains and the Urshen River (about 220 km long) flowing from the western part of the Great Hinggan Range (Xu et al., 1989).

Hulun Lake is in the semi-arid region of the middle temperate zone. The climate of the region is controlled by the East Asian Summer Monsoon (EASM) and continental polar air masses. Summers are short and warm and winters are long and cold (Xu et al., 1989). The regional mean annual temperature ranges from -0.7 to

1.1 °C, with a July average of 18.3 to 20.1 °C and a January average of -21.3 to -19.3 °C. Mean annual precipitation ranges from 248 to 292 mm, with 70% falling in summer (June-July-August). Mean annual evaporation ranges from 1500 to 1800 mm (Yan et al., 2012).

The modern natural vegetation of the Hulun Lake catchment is middle temperate steppe, and the plant communities consist mainly of *Stipa grandis*, *Stipa krylovii* and *Leymus chinensis* grass steppe, dominated by Gramineae, Asteraceae and Rosaceae species. The intrazonal vegetation includes psammophytes growing on the eastern shore of Hulun Lake and in the Chagang sandy land. Halophytes are distributed in the lowland areas or in areas with alkaline saline soils, and meadow occurs in the river valleys and wetlands (Inner Mongolia–Ningxia Integrated Survey Team, Chinese Academy of Sciences, 1985). On the western slopes of the Great Hinggan Range, coniferous forest is prevalent above 1000 m; it is dominated by *Larix gmeliiai*, *Betula platyphylla* and *Populus davidiana*, *Pinus pumila*, *Pinus sylvestris* and *Picea koraiensis* which occur sporadically. Between 800 and 1000 m, the vegetation is forest steppe with mesophytic meadows, with the sporadic occurrence of islands of birch and poplar forest and dense shrub land (Inner Mongolia–Ningxia Integrated Survey Team, Chinese Academy of Sciences, 1985). On the eastern slopes of the Hentiy Mountains, subalpine meadow occurs above 2000 m and is composed of cryophilous species (mainly of Cyperaceae, Asteraceae and Polygonaceae); between 1600 m and 2000 m, coniferous forest is present, dominated by *Larix sibirica* with the frequent occurrence of *Betula platyphylla*, *Picea obovata* and *Pinus sylvestris*. A forest-steppe belt occurs from 800 to 1600 m, with Gramineae, *Artemisia* spp., Chenopodiaceae, *Populus* spp. and *Ulmus pumila* (Hilbig, 1995).

3. Materials and methods

3.1. Core HL08

In January 2008, drilling was conducted on the ice at the depocenter of Hulun Lake using a TOHO (Japan) drilling system (Model D1-B). Sediment cores were extracted to a maximum depth of 921 cm beneath the lake floor and are designated HL08 (49°06'52.4"N, 117°31'56.0"E) (Fig. 1C). The core sections were split, photographed and described on site and then cut into 1-cm segments, resulting in 921 samples.

3.2. ^{14}C dating

Bulk samples were collected from organic-rich horizons from the upper 375 cm of core HL08 for accelerator mass spectrometry (AMS) ^{14}C dating. All samples were measured with a Compact-AMS system (NEC Pelletron) by Paleo Labo Co., Ltd (Japan). Organic carbon was extracted from each sample and dated following the methods described by Nakamura et al. (2000).

3.3. Pollen analysis

Pollen grains were extracted using a modified HCl-NaOH-HF procedure (Fægri et al., 1989). Before pretreatment, one tablet of *Lycopodium* spores (27,637 ± 563 grains) was added to each sample to calculate the pollen concentration. Pollen identifications were made under an Olympus BX 41 microscope with the aid of the *Pollen Flora of China* (Wang et al., 1995) and *Palynomorphs of Japanese Plants* (Shimarkura, 1973). More than 600 terrestrial pollen grains were counted for each sample.

Pollen percentages of terrestrial plants were based on the sum of total terrestrial pollen grains, while the percentages of aquatic pollen types and fern spores were based on the sum of terrestrial

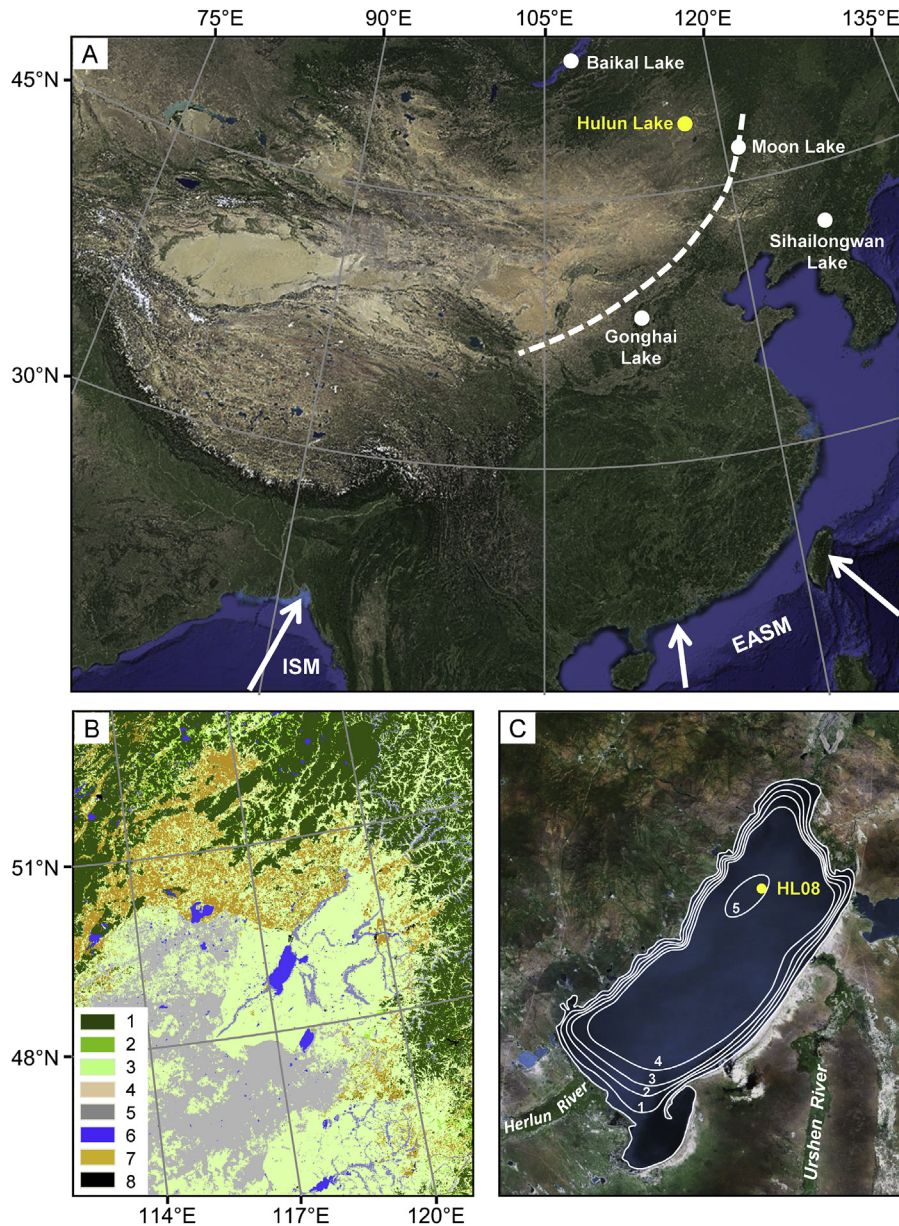


Fig. 1. A. Map of East Asia showing the current northern limit of the East Asian summer monsoon and the locations of the sites mentioned in the text. B. Vegetation of the Hulun Lake region (1. tree-covered areas, 2. shrub-covered areas, 3. grassland, 4. meadow, 5. sparse vegetation and bare soil, 6. waterbodies, 7. cropland, 8. artificial surfaces). C. Satellite image of Hulun Lake showing the location of core HL08; the bathymetric survey of the lake was conducted in July 2005 (contours in m). Satellite images are from <http://www.earth.google.com>; vegetation map modified from Global Land Cover-SHARE (<http://www.glcnc.org/>).

pollen grains plus the sum of aquatic pollen grains or fern spores. A pollen diagram was plotted using Tilia 1.7.16 and pollen assemblage zones were defined based on stratigraphically constrained cluster analysis (CONISS) (Grimm, 2011).

4. Results

4.1. Lithology and chronology

Core HL08 comprises a continuous sequence of lacustrine sediments without signs of hiatuses. It can be divided into three lithological units, as follows: 921–591 cm, greenish-grey clay and clayey silt; 591–375 cm, greenish-grey silt with gravel at the depths of 531–540 cm and 488–402 cm; 375–0 cm, greenish-grey clay and silt.

The vegetation history of the Hulun Lake region during the Holocene was reconstructed from core HL06 by Wen et al. (2010), and pollen assemblage of core HL08 produced consistent results with core HL06 during the Holocene. Here, we focus on the regional vegetation history of the Hulun Lake region during the last deglaciation (16,500–11,000 cal yr BP) that corresponds to the depths of 345–201 cm in core HL08 (Fig. 2A). The lithology of the depths of 345–201 cm in core HL08 can be divided into five lithological units, as follows: 345–313 cm, grey clayey sand; 313–284 cm, greenish-grey clayey silt; 284–260 cm, greenish-grey clay; 260–220 cm, greenish-grey clayey sand; 220–201 cm, greenish-grey sand.

As shown in Table 1, the uppermost 0–1 cm of the core has a ^{14}C age of 419 yr, which is likely the result of “hard-water” and other reservoir effects (Wen et al., 2010) and is here assumed to be roughly constant through the core. To obtain a realistic age–depth

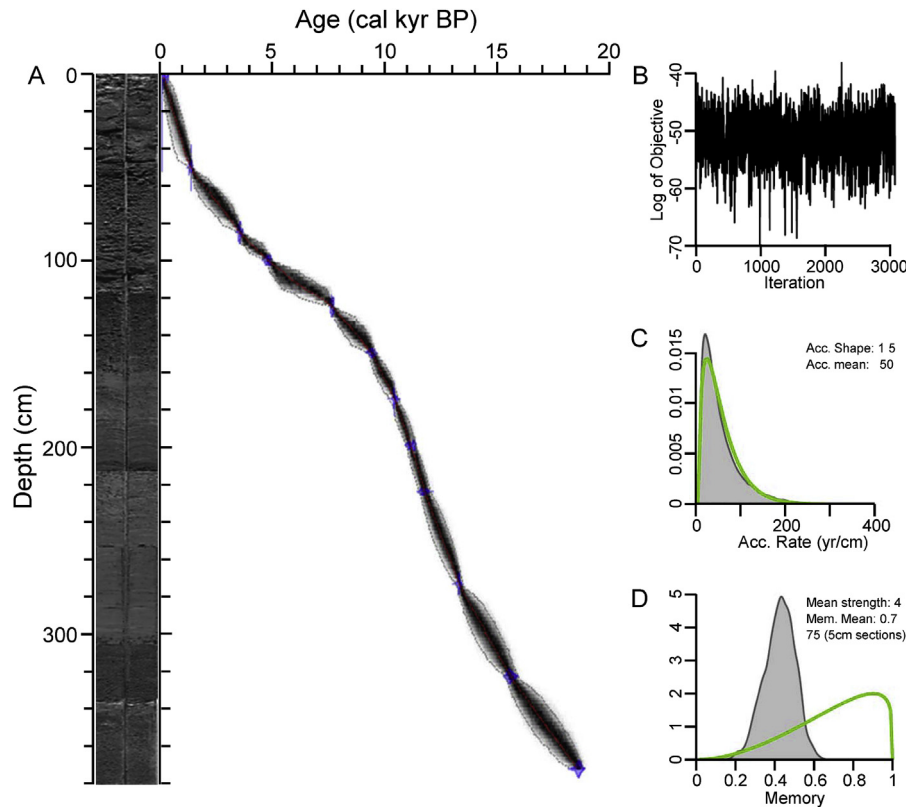


Fig. 2. Age-depth model for the upper 3.75 m of core HL08 from Hulun Lake. A. Calibrated ^{14}C dates (blue, with 2σ errors) and the age-depth model (darker grey shading indicates the more likely calendar ages; grey stippled lines show 95% confidence intervals; red curve shows the single 'best' model based on the weighted mean age for each depth). B. Number of Markov Chain Monte Carlo (MCMC) iterations used to generate the gray-scale graphs. C. Prior (green) and posterior (gray) distributions of the sediment accumulation rates (mean sediment accumulation rate is 50 yr/cm). D. Prior (green) and posterior (gray) distributions of memory (dependence of the sediment accumulation rate between neighboring depths). (For interpretation of the references to colour in this figure legend, the reader is referred to the Web version of this article.)

Table 1
AMS ^{14}C radiocarbon dates of samples from the upper 375 cm of core HL08.

NO. ^a	Depth (cm)	$\delta^{13}\text{C}$ ‰	AMS ^{14}C age yr BP	Corrected ^{14}C age ^b yr BP	Calibration age (2σ) cal. yr BP
PLD-13834	0–1	-27.45 ± 0.21	419 ± 20	0 ± 28	34–71
PLD-13837	49–50	-26.06 ± 0.13	1759 ± 20	1340 ± 28	1238–1304
PLD-14514	84–85	-25.06 ± 0.14	3638 ± 24	3219 ± 31	3372–3484
PLD-13839	99–100	-25.51 ± 0.21	4545 ± 24	4126 ± 31	4530–4727
PLD-13840	124–125	-25.82 ± 0.14	7018 ± 25	6599 ± 32	7434–7522
PLD-14515	149–150	-27.69 ± 0.21	8691 ± 33	8272 ± 39	9129–9410
PLD-13842	174–175	-27.05 ± 0.12	9515 ± 33	9096 ± 39	10192–10299
PLD-13843	199–200	-25.63 ± 0.12	10069 ± 30	9650 ± 36	11065–11190
PLD-13844	224–225	-25.11 ± 0.19	10456 ± 32	10037 ± 38	11386–11751
PLD-13846	274–275	-27.95 ± 0.17	11644 ± 36	11225 ± 41	13018–13167
PLD-13848	324–325	-25.05 ± 0.13	13283 ± 37	12864 ± 42	15177–15570
PLD-13850	374–375	-26.49 ± 0.12	15538 ± 48	15119 ± 52	18188–18558

^a PLD: Laboratory code of Paleo Labo Co., Ltd. (Japan).

^b Calibrated ages of reservoir-corrected radiocarbon dates. The reservoir correction factor is 419 yr (the ^{14}C age of the uppermost 1 cm of sediment core HL08). The weighted uncertainty is the root of the sum of squares of the errors of the AMS ^{14}C ages and reservoir ^{14}C ages.

model, we first subtracted the reservoir age of 419 yr from the original ^{14}C ages and then converted the resulting ages to calibrated ages using the OxCal 4.3 age calibration program (Bronk Ramsey, 2017) with the IntCal13 calibration data (Reimer et al., 2013). A Bayesian Accumulation Model was used to establish an age–depth profile (Blaauw and Christen, 2011). The upper 375 cm of the core HL08 was divided into 75 vertical sections of 5 cm thickness each. Prior settings for the accumulation rates were prescribed by a gamma distribution with a mean of ~ 50 yr/cm, and the dependence of the accumulation rate between neighboring depths was

moderate, indicating relatively stable accumulation (Fig. 2C&D). Accordingly, we calculated the age of each sampled horizon at 95% confidence intervals for the upper 375 cm of the core and then took the weighted mean age as the final age. The age–depth model for core HL08 is shown in Fig. 2A. The age of the base of the core is 18.3 kyr BP. The sediment accumulation rate is relatively rapid from 18.3 to 10 kyr BP, decreases significantly after 10 kyr BP and increases from 2 kyr to the present; during the last deglaciation, the sediment accumulation rate is ~ 26 cm/kyr.

4.2. Pollen assemblages

The pollen percentage diagram for core HL08 is illustrated in Fig. 3. A total of 69 fossil pollen and spore types were identified in 145 samples with 40 years resolution during the last deglaciation (345–201 cm, 16,500–11,000 cal yr BP). The arboreal pollen was dominated by *Pinus*, *Picea* and *Betula*; and the herbaceous pollen by *Artemisia*, Chenopodiaceae and Gramineae, followed by Cyperaceae, Asteraceae and *Thalictrum*. A relatively small number of fern spore and aquatic pollen types were also identified. The record can be divided into four zones based on CONISS analysis of terrestrial pollen percentages which are described below.

4.2.1. Pollen zone 1 (345–315 cm, 16,500–14,900 cal yr BP)

This zone is dominated by herbaceous pollen (up to 94%), accompanied by high frequencies of Chenopodiaceae (up to 34%), followed by *Artemisia* (up to 29%), Cyperaceae (up to 14%), Gramineae (up to 9%) and Asteraceae (up to 5%). Arboreal pollen frequencies, mainly *Betula* and *Picea*, are very low. The total pollen concentration is the lowest throughout the interval of study (~20,000 grains/gram).

4.2.2. Pollen zone 2 (314–284 cm, 14,900–13,500 cal yr BP)

The frequencies of *Betula*, *Artemisia* and *Thalictrum* increase very rapidly in this zone, by 10%, 15% and 5%, respectively. Chenopodiaceae decreases gradually (by ~18%), and Cyperaceae and Asteraceae also decrease slightly. The concentration of both arboreal and herbaceous pollen increases.

4.2.3. Pollen zone 3 (283–239 cm, 13,500–12,000 cal yr BP)

This zone is characterized by increases in arboreal pollen and decreases in herbaceous pollen. The frequencies of *Picea*, *Pinus*, *Larix* and *Alnus* increase significantly, while that of *Betula* is little changed. The frequencies of both *Artemisia* and Chenopodiaceae decrease by more than 10%, and those of Gramineae and Cyperaceae increase by ~5%. There is a striking decrease in the concentration of arboreal and herbaceous pollen.

4.2.4. Pollen zone 4 (238–201 cm, 12,000–11,000 cal yr BP)

The frequencies of *Picea* and *Pinus* decrease significantly in this zone, but *Betula* is largely unchanged. *Artemisia* and Chenopodiaceae increase by 15% and 5%, respectively, and Cyperaceae, Gramineae and Asteraceae decrease. The total pollen concentration is the highest throughout the studied interval (~160,000 grains/gram).

5. Discussion

5.1. Pollen source area and vegetational implications of the pollen assemblages from Hulun Lake

Hulun is a large lake with inflowing rivers and therefore we infer that, in addition to wind transport, pollen transport and input via rivers and streams is likely to be important. Today, *Larix* spp. and *Betula* spp. dominate the mixed coniferous-deciduous forest distributed on the western slopes of the Great Hinggan Range; Cyperaceae spp. and Asteraceae spp. dominate the vegetation of the subalpine meadows; *Pinus* spp., *Picea* spp. and *Betula* spp. dominate

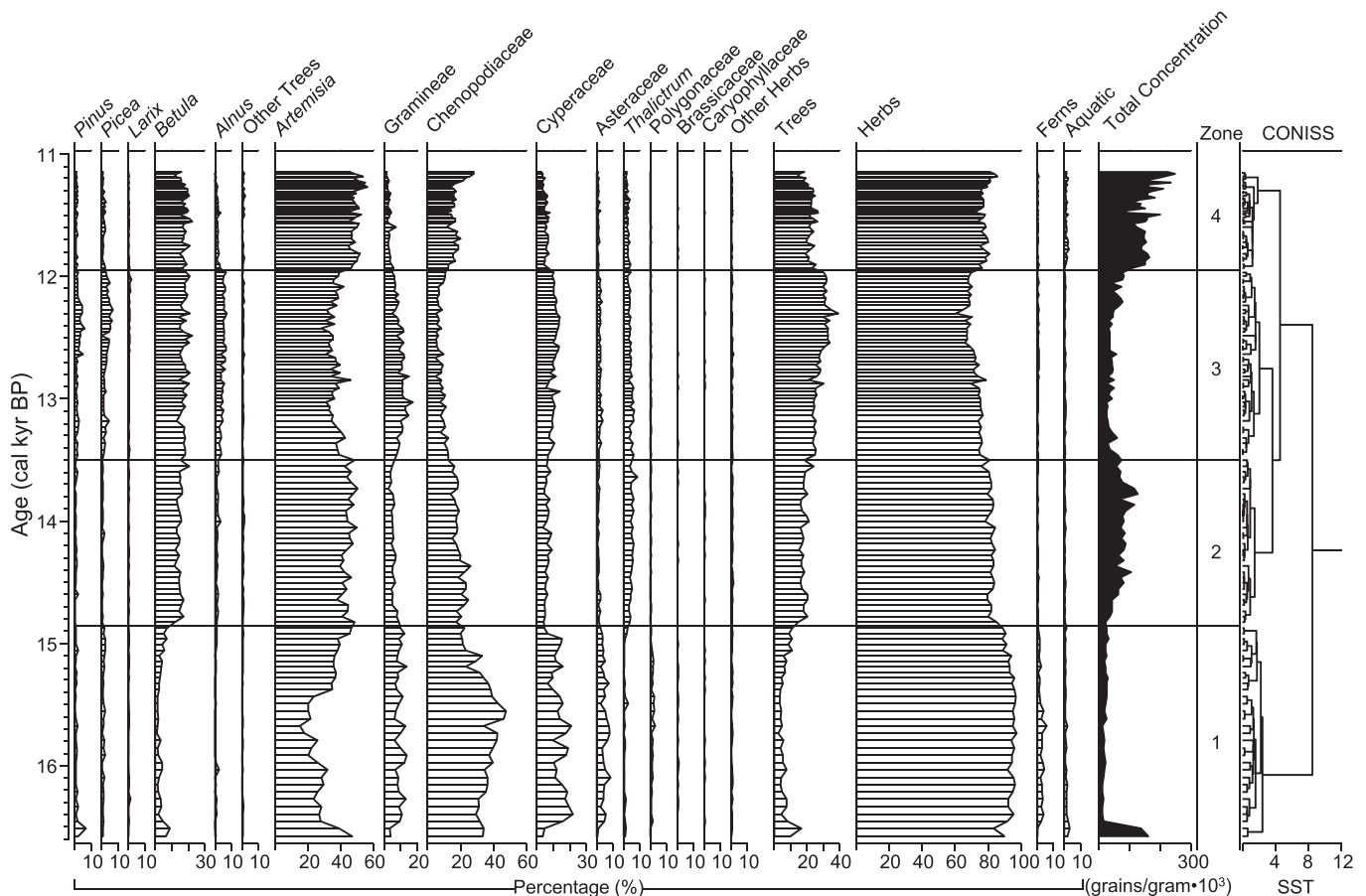


Fig. 3. Percentage pollen diagram for core HL08 spanning the last deglaciation (16,500–11,000 cal yr BP). Pollen assemblage zones are based on CONISS analysis.

the mixed coniferous-deciduous forest developed on the eastern slopes of the Hentiy Mountains; and Gramineae and *Artemisia* spp. dominate the typical steppe near the lake basin (Fig. 1B). Accordingly, we infer that the arboreal and subalpine meadow pollen types are mainly derived from the surrounding mountains and consequently reflect changes in mountain vegetation; while the herbaceous pollen types are of local origin and represent the vegetation in and around the lake basin.

To better understand the history of the regional vegetation around Hulun Lake during the last deglaciation, we combined the major pollen types into five ecological groups (Fig. 4): (1) Deciduous forest, including thermophilic arboreal pollen types such as *Betula*, *Quercus*, and *Ulmus*, and cryophilous deciduous arboreal and shrub pollen types such as *Alnus* and *Spiraea*. (2) Coniferous forest, consisting of coniferous pollen types such as *Pinus*, *Picea*, *Larix* and Cupressaceae. (3) Subalpine meadow, including cryophilous herb pollen types such as Cyperaceae (*Kobresia* and *Carex*), Asteraceae, Caryophyllaceae and Polygonaceae. (4) Typical steppe, mainly comprising mesophytic herb pollen types such as *Artemisia* and Gramineae, and hygrophilous herb pollen types. (5) Desert steppe, consisting of xerophytic herb pollen types such as Chenopodiaceae, *Ephedra* and *Hippophae*. Changes in the deciduous forest, coniferous forest and subalpine meadow groups likely reflect vegetation succession within the surrounding mountains; and those of the typical steppe and desert steppe groups likely reflect vegetation change within the lake catchment and close to the lake basin.

5.2. Vegetation succession within the Hulun Lake region during the last deglaciation

The regional vegetation around Hulun Lake changed

dramatically during the last deglaciation, from subalpine meadow-desert steppe to mixed coniferous and deciduous forest-typical steppe. Based on the variations of the major ecological groups, the regional vegetation history during this time are coincident with the H1 event, the B/A warming, the YD event and the early Holocene period occurred in high northern latitudes. The vegetation changes within and between these intervals are discussed below.

5.2.1. The H1 event

The low representation of the deciduous and coniferous forest groups and high representation of the subalpine meadow group indicates the mosaic-like occurrence of subalpine meadow and sparse woodland. The proportion of typical steppe was the lowest during the deglaciation and Chenopodiaceae-denominated desert steppe developed, suggesting that the immediate area around the lake basin was occupied by desert steppe. Overall, the regional vegetation cover was sparse.

5.2.2. The Bølling-Allerød warming

This interval was characterized by the rapid expansion of pioneer trees (*Betula* spp.) and decreases in the proportion of both the coniferous forest and subalpine meadow groups, indicating the rapid expansion of deciduous forest and an increase in the density of forest cover in the mountains. The marked increases in the proportion of mesophytic and hygrophilous herbaceous plants indicates the gradual replacement of desert steppe by *Artemisia*-dominated typical steppe. Overall, the regional vegetation cover increased.

5.2.3. The Younger Dryas event

Betula-dominated deciduous forest remained the predominant

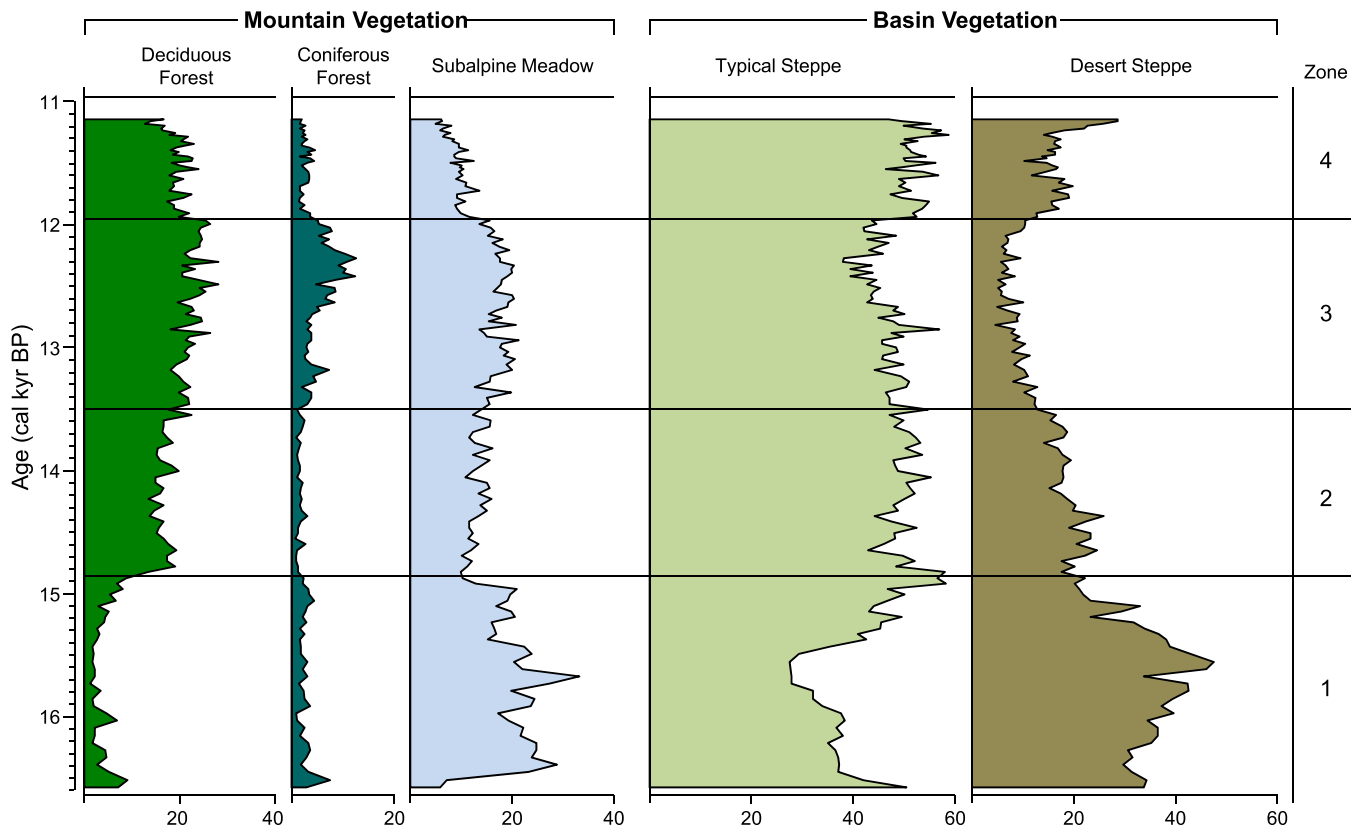


Fig. 4. Variation of pollen ecological groups for core HL08 during the last deglaciation (16,500–11,000 cal yr BP). The pollen ecological group zones are based on pollen assemblage zones.

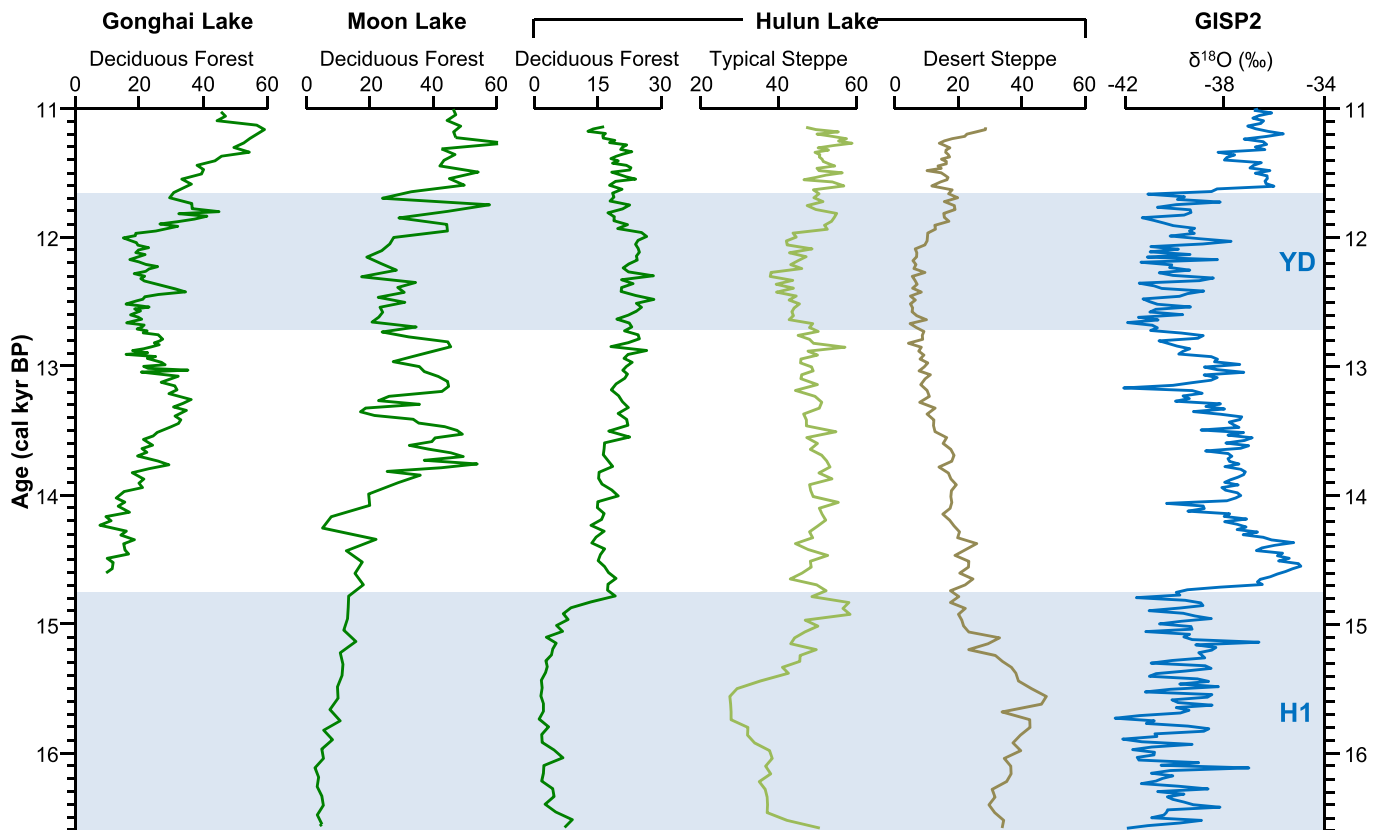


Fig. 5. Comparison of major regional vegetation composition (deciduous forest, typical steppe and desert steppe) of core HL08 from Hulun Lake during the last deglaciation (16,500–11,000 cal yr BP) with deciduous forest records from Gonghai Lake (Xu et al., 2017) and Moon Lake (Wu et al., 2016a), and the $\delta^{18}\text{O}$ record from the Greenland Ice Sheet Project 2 (GISP2) ice core (Stuiver and Grootes, 2000). Heinrich event 1 (H1) and the Younger Dryas event (YD) are indicated by a light blue background. (For interpretation of the references to colour in this figure legend, the reader is referred to the Web version of this article.)

mountain vegetation type in the mountains. However, at the same time coniferous forest (including *Pinus*, *Picea* and *Larix*) reach its maximum representation, indicating the occurrence of mixed coniferous-deciduous forest in and around the surrounding mountains. In addition, the proportion of subalpine meadow increased slightly, suggesting a reduced forest cover and presence of relatively open landscapes in mountains. Around the lake basin, the regional ecological environment deteriorated and the vegetation cover was reduced compared to the B/A warming event; however, the regional vegetation remained typical steppe.

5.2.4. The early Holocene

The high frequencies of thermophilous trees (*Quercus* spp. and *Ulmus* spp.) and the marked decreases in the proportions of coniferous forest and subalpine meadow suggest the re-expansion of deciduous forest and decline of coniferous forest. In addition, the high arboreal pollen concentration indicates the establishment of dense forest cover around the surrounding mountains. Typical steppe occupied the area around the lake basin, implying an overall increase in the density of the vegetation cover.

5.3. Differential response of the regional vegetation to the H1 and YD events

The H1 and YD events were the most prominent cooling events in the North Atlantic region during the last deglaciation, and had a profound influence on global atmospheric circulation and terrestrial ecosystems (Denton et al., 2010; Clark et al., 2012). Oxygen isotope records from the Greenland ice core (GISP2, Stuiver and

Grootes, 2000, Fig. 5) and sea surface temperature (SST) records in the North Atlantic (core SU8188, Bard et al., 2000) indicate that climatic conditions were comparable during H1 and the YD in the North Atlantic region. However, at Hulun Lake the response of the regional vegetation to the H1 and YD events was significantly different (Fig. 5). During the interval of H1, the regional vegetation consisted mainly of herbaceous plants (>90% of total pollen) and the proportion of deciduous forest was extremely low, indicating that the catchment was occupied by Chenopodiaceae-dominated desert steppe, that the vegetation cover was sparse, and that there was intense aeolian activity (Zeng et al., 2013). In contrast during the YD event, forest was well developed in the surrounding mountains, with the proportion of deciduous forest pollen types comprising up to 20% of the terrestrial pollen; at the same time, *Artemisia*-dominated typical steppe occupied the catchment and the vegetation cover was relatively dense.

Pollen records from other lake sites in the northern margin of Asian summer monsoon (Fig. 5), also highlight the differential response of regional vegetation to the H1 and YD events. Herbaceous plants (mainly *Artemisia*, Chenopodiaceae, Asteraceae and Cyperaceae) dominated the regional vegetation (60–90%) of Sihailongwan Lake (Stebich et al., 2009), Moon Lake (Wu et al., 2016a) and Lake Baikal (Demske et al., 2005) during H1, suggesting that the forest density and overall vegetation cover were low at the northern margin of Asian summer monsoon. During the YD event, the proportion of arboreal pollen reached 24% in Gonghai Lake (Xu et al., 2017), and increased by ~20%, ~18% and ~40%, respectively, at Sihailongwan Lake (Stebich et al., 2009), Moon Lake (Wu et al., 2016a) and Lake Baikal (Demske et al., 2005) compared

to the H1 event. The vegetation was dominated by pioneer trees (*Betula* spp.) with *Picea* spp. and *Larix* spp., indicating that deciduous forest was relatively well developed and the density of forest cover increased in the northern margin of Asian summer monsoon, compared to the interval of H1.

Climatic conditions (temperature and precipitation) are the most important limiting factors for vegetation development. We suggest that changes in Northern Hemisphere summer insolation and land surface conditions (ice sheets and sea level) were responsible for the variations in temperature and monsoonal precipitation that were the main cause of the differential response of the regional vegetation to the H1 and YD events around Hulun Lake and elsewhere. During the H1 event, summer insolation in the Northern Hemisphere was low (Laskar et al., 2004) and the mean latitudinal position of the intertropical convergence zone (ITCZ) shifted southwards and the Asian summer monsoon weakened due to the collapse of the Atlantic meridional overturning circulation (AMOC) (McManus et al., 2004). In addition, the existence of the remnant Northern Hemisphere ice sheets suppressed the northward shift of the summer monsoon rain belt (Dyke, 2004), thus leading to dramatic cooling and drying in the northern margin of the Asian summer monsoon, and triggering significant vegetation changes. During the YD event, in contrast, summer insolation in the Northern Hemisphere increased (Laskar et al., 2004) and the mean annual temperature of the Northern Hemisphere was higher than during the H1 event (Shakun et al., 2012), leading to a northward shift of the ITCZ and the strengthening of the Asian summer monsoon. In addition, the extent of the monsoon moisture source area was extended due to the reduction in the remnant Northern Hemisphere ice sheets (Dyke, 2004) and the rise of global sea level (Lambeck et al., 2014); thus, more monsoon precipitation was supplied to the northern margin of Asian summer monsoon than during H1 (Clark et al., 2012). In addition, the nature of the pre-existing vegetation, the extent of permafrost and the intensity of blown-sand activities may also have contributed to the differential response of the regional vegetation to the two climatic events: The vegetation composition and community structure were different in the northern margin of Asian summer monsoon (e.g., Lake Baikal - Demske et al., 2005; Sihailongwan Lake - Stebich et al., 2009; Moon Lake - Wu et al., 2016a, 2016b) during the Last Glacial Maximum (LGM) and B/A warming, and this may have resulted in differences in the character of retrogressive succession of the regional vegetation during the H1 event and YD event; Meanwhile, the extent of permafrost was much larger, and the intensity of blown-sand activities was more intense during the H1 event than that during the YD event (Zeng et al., 2013; Zhao et al., 2014; Jin et al., 2016), which may also have affected the soil conditions (include moisture, temperature and fertility) and distribution of plant species during the H1 event and YD event. Therefore, the development of quantitative methods of evaluating the response of vegetation to climate change and the role of vegetation succession and background conditions are important topics that needs to be addressed in future global change research.

Comparison of the modern pollen spectra from the top of core HL06 from Hulun Lake (Wen et al., 2010) and the fossil pollen spectra from core HL08 shows that the modern pollen assemblages are analogous to those spanning the B/A warming interval, indicating that the modern regional vegetation composition is similar to that during the B/A interval. Therefore, it is possible that the impact of possible extreme climatic events on the regional vegetation of the Hulun Lake region may be analogous to that of the YD event under future global warming scenarios: Deciduous forest would dominate the surrounding mountains; there would be a marked increase in coniferous forest and a decrease in overall forest cover; the extent and vegetation density of typical steppe would be

gradually reduced; and there would be a gradual deterioration of the regional ecological environment.

6. Conclusions

A high-resolution (~40 yr) pollen record provides a detailed history of regional vegetation change in the climatically sensitive Hulun Lake region during the last deglaciation (16,500–11,000 cal yr BP). During the cold H1 event and YD event, coniferous forest and subalpine meadow developed in the mountains, Chenopodiaceae-dominated desert steppe occupied the lake catchment and the overall regional vegetation density was low. In contrast, during the warm B/A event and the early Holocene, mixed coniferous-deciduous forest expanded in the mountains, typical steppe occupied the lake catchment, and the overall vegetation cover was dense. However, the responses of the regional vegetation to the cold H1 and YD events were significantly different, mainly manifested as differences in the forest cover in the mountains and the vegetation composition of the lake catchment. We conclude that differences in Northern Hemisphere summer insolation and in land surface conditions (ice sheets and sea level) were responsible for the differences in temperature and monsoonal precipitation variations which resulted in the contrasts in vegetation composition. Based on the observed vegetation responses we suggest that extreme climatic events under future global warming scenarios may result in a deterioration of the ecological environment of the Hulun Lake region.

Acknowledgements

We sincerely thank two anonymous reviewers for valuable comments and suggestions. This work was supported by the National Key R&D Program of China (grant numbers 2017YFA0603403) and the National Natural Science Foundation of China (grant numbers 41672166). We thank Dr. Jan Bloemendal for improving the English language.

References

- Bard, E., Rostek, F., Turon, J.L., Gendreau, S., 2000. Hydrological impact of Heinrich events in the subtropical northeast Atlantic. *Science* 289 (5483), 1321–1324.
- Binney, H., Edwards, M., Macias-Fauria, M., Lozhkin, A., Anderson, P., Kaplan, J.O., Andreev, A., Bezrukova, E., Blyakharchuk, T., Jankovska, V., Khazina, I., Krivonogov, S., Kremenetski, K., Nield, J., Novenko, E., Ryabogina, N., Solovieva, N., Willis, K., Zernitskaya, V., 2017. Vegetation of Eurasia from the last glacial maximum to present: key biogeographic patterns. *Quat. Sci. Rev.* 157, 80–97.
- Blaauw, M., Christen, J.A., 2011. Flexible paleoclimate age-depth models using an autoregressive gamma process. *Bayesian Anal.* 6 (3), 457–474.
- Bonan, G.B., Pollard, D., Thompson, S.L., 1992. Effects of boreal forest vegetation on global climate. *Nature* 359 (6397), 716–718.
- Bronk Ramsey, C., 2017. OxCal Program Version 4.3. University of Oxford Radiocarbon Accelerator Unit, Oxford.
- Clark, P.U., Shakun, J.D., Baker, P.A., Bartlein, P.J., Brewer, S., Brook, E., Carlson, A.E., Cheng, H., Kaufman, D.S., Liu, Z.Y., Marchitto, T.M., Mix, A.C., Morrill, C., Otto-Bliesner, B.L., Pahnke, K., Russell, J.M., Whitlock, C., Adkins, J.F., Blois, J.L., Clark, J., Colman, S.M., Curry, W.B., Flower, B.P., He, F., Johnson, T.C., Lynch-Stieglitz, J., Markgraf, V., McManus, J., Mitrovica, J.X., Moreno, P.I., Williams, J.W., 2012. Global climate evolution during the last deglaciation. *Proc. Natl. Acad. Sci. U. S. A.* 109 (19), E1134–E1142.
- Demske, D., Heumann, G., Granoszewski, W., Nita, M., Mamakowa, K., Tarasov, P.E., Oberhänsli, H., 2005. Late Glacial and Holocene vegetation and regional climate variability evidenced in high-resolution pollen records from Lake Baikal. *Glob. Planet. Change* 46 (1–4), 255–279.
- Denton, G.H., Anderson, R.F., Toggweiler, J.R., Edwards, R.L., Schaefer, J.M., Putnam, A.E., 2010. The last glacial termination. *Science* 328 (5986), 1652–1656.
- Dyke, A.S., 2004. An outline of North American deglaciation with emphasis on central and northern Canada. *Dev. Quat. Sci.* 2 (B), 373–424.
- Dyke, A.S., 2005. Late quaternary vegetation history of northern North America based on pollen, macrofossil and faunal remains. *Geogr. Physique Quaternaire* 59, 211–262.
- Fægri, K., Kaland, P.E., Krzywinski, K., 1989. *Textbook of Pollen Analysis*, fourth ed. John Wiley and Sons, Chichester, pp. 1–328.

- Grimm, E.C., 2011. Tilia Version 1.7.16. Illinois State Museum, Illinois.
- Hilbig, W., 1995. The Vegetation of Mongolia. SPB Academic Publishing, Amsterdam, pp. 1–257.
- Hughen, K.A., Eglinton, T.I., Xu, L., Makou, M., 2004. Abrupt tropical vegetation response to rapid climate changes. *Science* 304 (5679), 1955–1959.
- Huntley, B., 1990. European post-glacial forests: compositional changes in response to climatic change. *J. Veg. Sci.* 1 (4), 507–518.
- Inner Mongolia–Ningxia Integrated Survey Team, Chinese Academy of Sciences, 1985. Vegetation of Inner Mongolia. Science Press, Beijing, pp. 1–884 (in Chinese).
- Jacobson, G.L., Bradshaw, R.H.W., 1981. The selection of sites for paleovegetational studies. *Quat. Res.* 16 (1), 80–96.
- Jin, H.J., Chang, X.L., Luo, D.L., He, R.X., Lv, L.Z., Yang, S.Z., Guo, D.X., Chen, X.M., Harris, S.A., 2016. Evolution of permafrost in northeast China since the late pleistocene. *Sci. Cold Arid Regions* 8 (4), 269–296.
- Lambeck, K., Rouby, H., Purcell, A., Sun, Y., Sambridge, M., 2014. sea level and global ice volumes from the last glacial maximum to the Holocene. *Proc. Natl. Acad. Sci. U. S. A.* 111 (43), 15296–15303.
- Lashof, D.A., Deangelo, B.J., Saleska, S.R., Harte, J., 1997. Terrestrial ecosystem feedbacks to global climate change. *Annu. Rev. Energy Environ.* 22 (1), 75–118.
- Laskar, J., Robutel, P., Joutel, F., Gastineau, M., Correia, A.C.M., Levrard, B., 2004. A long-term numerical solution for the insolation quantities of the earth. *Astronomy Astrophysics* 428 (1), 261–285.
- Mcmannus, J.F., Francois, R., Gherardi, J.M., Keigwin, L.D., Brown-Leger, S., 2004. Collapse and rapid resumption of Atlantic meridional circulation linked to deglacial climate changes. *Nature* 428 (6985), 834–837.
- Nakamura, T., Niu, E., Oda, H., Ikeda, A., Minami, M., Takahashi, H., Adachi, M., Pals, L., Gottang, A., Suya, N., 2000. The HVEE tandem AMS system at nagoya university. *Nucl. Instrum. Methods Phys. Res. B* 172, 52–57.
- Park, J., Park, J., 2015. Pollen-based temperature reconstructions from Jeju Island, South Korea and its implication for coastal climate of East Asia during the late Pleistocene and early Holocene. *Palaeogeogr. Palaeoclimatol. Palaeoecol.* 417, 445–457.
- Prentice, I.C., Bartlein, P.J., Webb, T., 1991. Vegetation and climate change in eastern North America since the last glacial maximum. *Ecology* 72 (6), 2038–2056.
- Reimer, P.J., Bard, E., Bayliss, A., Beck, J.W., Blackwell, P.G., Bronk Ramsey, C., Buck, C.E., Cheng, H., Edwards, R.L., Friedrich, M., Grootes, P.M., Guilderson, T.P., Hafflidason, H., Hajdas, I., Hatté, C., Heaton, T.J., Hoffmann, D.L., Hogg, A.G., Hughen, K.A., Kaiser, K.F., Kromer, B., Manning, S.W., Niu, M., Reimer, R.W., Richards, D.A., Scott, E.M., Southon, J.R., Staff, R.A., Turney, C.S.M., van der Plicht, J., 2013. IntCal13 and Marine13 radiocarbon age calibration curves 0–50,000 years cal BP. *Radiocarbon* 55 (4), 1869–1887.
- Schimmel, D.S., 1995. Terrestrial ecosystems and the carbon cycle. *Glob. Change Biol.* 1 (1), 77–91.
- Shakun, J.D., Clark, P.U., He, F., Marcott, S.A., Mix, A.C., Liu, Z.Y., Otto-Bliesner, B., Schmittner, A., Bard, E., 2012. Global warming preceded by increasing carbon dioxide concentrations during the last deglaciation. *Nature* 484 (7392), 49–54.
- Shimarkura, M., 1973. Palynomorphs of Japanese Plants, vol. 5. Special publication of the Osaka Museum of Natural History, Osaka (in Japanese).
- Stebich, M., Mingram, J., Han, J.T., Liu, J.Q., 2009. Late Pleistocene spread of (cool-) temperate forests in Northeast China and climate changes synchronous with the North Atlantic Region. *Glob. Planet. Change* 65, 56–70.
- Stuiver, M., Grootes, P.M., 2000. GISP2 oxygen isotope ratios. *Quat. Res.* 53, 277–284.
- Sugita, S., 1994. Pollen representation of vegetation in Quaternary sediments: theory and method in patchy vegetation. *J. Ecol.* 82 (4), 881–897.
- Wang, F.X., Chien, N.F., Zhang, Y.L., Yang, H.Q., 1995. Pollen Flora of China, second ed. Science Press, Beijing, pp. 1–461 (in Chinese).
- Wen, R.L., Xiao, J.L., Chang, Z.G., Zhai, D.Y., Xu, Q.H., Li, Y.C., Itohc, S., Lomtatidze, Z., 2010. Holocene climate changes in the mid-high-latitude- monsoon margin reflected by the pollen record from Hulun Lake, northeastern Inner Mongolia. *Quat. Res.* 73 (2), 293–303.
- Williams, J.W., Post, D.M., Cwynar, L.C., Lotter, A.F., Levesque, A.J., 2002. Rapid and widespread vegetation responses to past climate change in the North Atlantic region. *Geology* 30 (11), 971–974.
- Wu, J., Liu, Q., Wang, L., Chu, G.Q., Liu, J.Q., 2016a. Vegetation and climate change during the last deglaciation in the Great khingan mountain, northeastern China. *PLOS One* 11 (1), e0146261.
- Wu, J., Liu, Q., Chu, G.Q., Wang, L., Liu, J.Q., 2016b. Vegetation history and climate change recorded by stomata evidence during the late glacial in the Great Khingan Mountain Region, Northeastern China. *Chin. Sci. Bull.* 61 (36), 3940–3945 (in Chinese with English Abstract).
- Xiao, J.L., Chang, Z.G., Wen, R.L., Zhai, D.Y., Itoh, S., Lomtatidze, Z., 2009. Holocene weak monsoon intervals indicated by low lake levels at Hulun Lake in the monsoonal margin region of northeastern Inner Mongolia, China. *Holocene* 19, 899–908.
- Xu, Q.H., Chen, F.H., Zhang, S.R., Cao, X.Y., Li, J.Y., Li, Y.C., Li, M.Y., Chen, J.H., Liu, J.B., Wang, Z.L., 2017. Vegetation succession and East Asian summer monsoon changes since the last deglaciation inferred from high-resolution pollen record in Gonghai Lake, shanxi province, China. *Holocene* 27 (6), 835–846.
- Xu, Z.J., Jiang, F.Y., Zhao, H.W., Zhang, Z.B., Sun, L., 1989. Annals of Hulun Lake. Jilin Literature and History Publishing House, Changchun, pp. 1–33 (in Chinese).
- Yan, M.H., Liu, S.T., Zhang, W., Zong, C., Lou, J., 2012. The Characteristics of Climate Change and its Influence on Ecological Environment of Hulun Lake. Science Press, Beijing, pp. 162–187 (in Chinese and English).
- Yu, Z., Eicher, U., 1998. Abrupt climate oscillations during the last deglaciation in central North America. *Science* 282, 2235–2238.
- Zeng, L., Lu, H.Y., Yi, S.W., Chen, Y.Y., Zhu, F.Y., 2013. Environmental changes of Hulun Buir Dune field in northeastern China during the last glacial maximum and Holocene optimum. *Quat. Sci.* 33 (2), 243–251 (in Chinese with English Abstract).
- Zhao, L., Jin, H., Li, C., Cui, Z., Chang, X., Marchenko, S.S., Vandenbergh, J., Zhang, T.J., Luo, D.L., Guo, D.X., Liu, G.N., Yi, C.L., 2014. The extent of permafrost in China during the local Last Glacial Maximum (LLGM). *Boreas* 43 (3), 688–698.